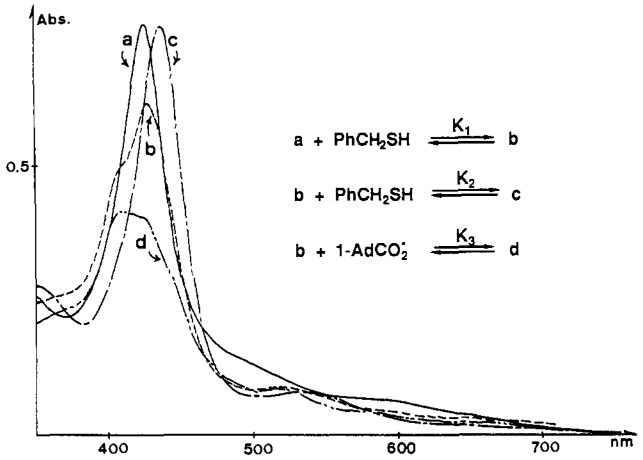

Figure 2. Electronic spectra of the ferric complex of **Ia**(**b**) in the aqueous phosphate buffer solution (pH = 7.0). (a) **Ia**(**b**)·Fe(III)·Cl; 6.3×10^{-6} M, (b) (a) + 6.3×10^{-6} M of benzylmercaptane, (c) (a) + 6.0×10^{-5} M of benzylmercaptane, (d) (b) + 6.0×10^{-5} M of 1-adamantanecarboxylate.

observed for an aromatic region where signals of pyrrole and benzene rings appeared;[5] i.e., two types of benzene protons at 3, 4, 5, and 6 positions and four types of pyrrole protons were observed for **Ie**; and, in contrast, all benzene and pyrrole protons appeared separately for **Id** (Figure 1 (parts b and c)). For **Ic**, the reduced signal pattern similar to that for **Ie** was observed because of its C_2 symmetry. In the case of **Ia** and **Ib**, the situations are somewhat different from those of **Ic–e**. Since, in these diagonal coupling products, the C_4 symmetry axis of the tetraphenylporphyrin part and the C_7 symmetry axes of two cyclodextrin parts almost coincide, 14 glucose rings in these compounds exist in the very similar environment. Thus, more heavily overlapped C1–H signals were observed for **Ia** and **Ib** as shown in Figure 1a, though spectra of the aromatic region are still analyzable as that of the molecule with C_2 symmetry. Combining these results of diagonal and side coupling patterns, statistical yields and elution patterns of each isomer in HPLC analyses,[6] and NMR spectra, the structures of present cyclodextrin-sandwiched porphyrins are assigned except **Ia** and **Ib**; i.e., for two diagonal coupling products, it is not determined at the present stage which product is corresponding to **Ia** or **Ib**.

As one of the examples of usefulness of the present cyclodextrin-sandwiched porphyrin that the hemoprotein mimics, the coordination and binding behavior of the Fe(III) complex of **Ia**(**b**) was preliminarily investigated.[7] The spectroscopic behavior of axial coordination by benzylmercaptane and binding of 1-adamantanecarboxylate in aqueous solution is shown in Figure 2. The titration experiments show the following characteristic behavior of the present Fe(III) complex: (i) tight first coordination by benzylmercaptane ($K_1 > 10^7$ M^{-1}, species b in Figure 2), (ii) second coordination by the mercaptane with the measurable binding constant ($K_2 = (7 \pm 3) \times 10^4$ M^{-1}, species c in Figure 2), (iii) binding of 1-adamantanecarboxylate with the usual binding constant ($K_3 = (7 \pm 1) \times 10^5$ M^{-1}, species d in Figure 2) which suggests that 1-adamantanecarboxylate can be bound more easily than the second benzylmercaptane molecule. The final observation is very interestingly related with the initial substrate binding step of P-450. It is well established for some cytochrome P-450's that the spin state of the ferric heme is largely affected by addition of substrate.[8] Thus, the species generated in step iii which has one mercaptane ligand and one hydrophobic adamantane molecule seems to be a promising model for investigation on these initial reaction steps of P-450.[9]

The more detailed investigations using present cyclodextrin-sandwiched porphyrines as hemoprotein mimics are now underway in our laboratory.

---

(5) Since the NMR signal of pyrrole protons of **Ic** and **Id** were very broad at 25 °C and sharpened at 80 °C, porphyrin rings of these compounds were expected to suffer significant motional restriction at room temperature.

(6) The order of retention times of these isomers in HPLC analyses is **Ie** > **Id** > **Ic** > **Ib**(**a**) ≥ **Ia**(**b**). This order is determined by the degree of positional deviations of two cyclodextrin molecules relative to the porphyrin ring, which alters the number of exposed C6–OH's, the exposed area of porphyrin surface, and the molecular dimension of **I**.

(7) The Fe(III) and Zn(II) metalation of **I** proceeds normally by using $FeCl_2$ and $Zn(Ac)_2$ in DMF-pyridine or 2,6-lutidine.

(8) *Cytochrome P-450*; Ortiz de Montellano, P. R., Ed.; Plenum Press: New York, 1986.

(9) Preliminary results of EPR measurements at 4 K show the generation of the high spin ferric species by addition of 1-adamantanecarboxylate.

Synthesis and Gas-Phase Vibrational Circular Dichroism of (+)-(*S*,*S*)-Cyclopropane-1,2-$^2H_2$

Steven J. Cianciosi, Kevin M. Spencer, Teresa B. Freedman,* Laurence A. Nafie,* and John E. Baldwin†

Department of Chemistry, Syracuse University
Syracuse, New York 13244-1200

Received September 26, 1988

Synthesis of (+)-(*S*,*S*)-cyclopropane-1,2-$^2H_2$ has been achieved only once, by Berson and Pedersen in 1974.[1] In spite of the evident utility offered by the chiral dideuteriocyclopropanes for fundamental spectroscopic and reactivity studies, they have remained largely a subject for theoretical conjecture rather than of experimental scrutiny. For example, in 1986, Lowe, Segal, and Stephens[2] predicted the vibrational circular dichroism (VCD)[3-7] spectrum of (+)-(*S*,*S*)-cyclopropane-1,2-$^2H_2$, but no VCD data for this exceptionally suitable subject were then or have subsequently been obtained.

We have responded to this situation by developing a new synthetic route to the chiral dideuteriocyclopropanes, preparing both antipodes in optically pure form as well as the racemic species, and securing gas-phase VCD spectra between 3100 and 850 cm^{-1}.

Dimethyl *trans*-cyclopropanedicarboxylate-1,2-$^2H_2$ was hydrolyzed[8] to the enantiomeric acid esters, which were resolved by way of the diastereomeric amides prepared from (−)-(*R*)-2-phenylglycinol.[9] Chromatography provided both diastereomeric ester amides of better than 99% diastereomeric purity. Each amide was hydrolyzed in aqueous H_2SO_4:THF, and the resulting diacids were converted to the corresponding dimethyl esters (96% deuterated at C(1,2) by NMR, >98 ee by Eu(hfc)$_3$ chiral shift reagent analysis, 57% yield from the (±)-d_2-diester). The d_2-diester from the early eluting amide had $[\alpha]_D$−239° ($CDCl_3$) and thus is of (*R*,*R*) configuration.[10,11] Each chiral d_2-diester was reduced to the corresponding d_2-dialdehyde ($^iBu_2AlH$, −100 °C); the gas

---

(1) Berson, J. A.; Pedersen, L. D. *J. Am. Chem. Soc.* **1975**, *97*, 238–240. Berson, J. A.; Pedersen, L. D.; Carpenter, B. K. *J. Am. Chem. Soc.* **1976**, *98*, 122–143.

(2) Lowe, M. A.; Segal, G. A.; Stephens, P. J. *J. Am. Chem. Soc.* **1986**, *108*, 248–256.

(3) Freedman, T. B.; Nafie, L. A. In *Topics in Stereochemistry*; Eliel, E. L., Wilen, S. H., Eds.; Wiley: New York, 1987; Vol. 17, pp 113–205.

(4) Nafie, L. A.; Freedman, T. B. *Spectroscopy* **1987**, *2*(*12*), 24–29.

(5) Stephens, P. J.; Lowe, M. A. *Annu. Rev. Phys. Chem.* **1985**, *36*, 213–241.

(6) Polavarapu, P. L. In *Vibrational Spectra and Structure*; Durig, J. R., Ed., Elsevier: Amsterdam, 1984; Vol. 13, pp 103–160.

(7) Keiderling, T. A. *Appl. Spectrosc. Rev.* **1981**, *17*, 189–226.

(8) Schneider, M.; Engel, N.; Boensmann, H. *Angew. Chem., Int. Ed. Engl.* **1984**, *23*, 64–66.

(9) Helmchen, B.; Nill, B.; Flockerzi, D.; Youssef, M. S. K. *Angew. Chem., Int. Ed. Engl.* **1979**, *18*, 62–65. Jaenicke, L.; Boland, W.; Schotten, T. *Helv. Chim. Acta* **1985**, *68*, 1186–1192.

(10) (a) Doering, W. von E.; Sachdev, K. *J. Am. Chem. Soc.* **1974**, *96*, 1168–1187. (b) Heintz, V. J.; Keiderling, T. A. *J. Am. Chem. Soc.* **1981**, *103*, 2395–2403.

(11) The (*R*,*R*)-d_0-diester had $[\alpha]_{578}$−233° (MeOH); lit.[10a] −232°; from the (*S*,*S*)-d_2-amide was secured diester of $[\alpha]_D$ +236 (CCl_4), +239° ($CDCl_3$); lit.[10b] +236° (CCl_4).

0002-7863/89/1511-1913$01.50/0 © 1989 American Chemical Society

Table I. Observed and Calculated Frequencies, Relative Intensities, and VCD Signs for the Normal Modes of (+)-(*S*,*S*)-Cyclopropane-1,2-$^2H_2$

symmetry species	observed		calculated[a]	
	freq (cm^{-1})	VCD	freq (cm^{-1})	VCD
B	3090 vs	(+) m	3105 s	(+) s
B	3057 vs	(−) s	3073 s	(−) vs
A	~3049 w	(+) m	3075 w	(+) s
A	3025 m	(+) m	3041 s	(+) s
A	2277 w	(−) s	2271 w	(−) s
B	2269 vs	(+) m	2260 s	(+) s
A	n.o.[b]	n.o.	1459 w	(+) w
A	1355 w	(−) m	1345 w	(−) s
B	1300 m	(+) m	1300 w	(+) s
A	1187 vw?	(+) vw?	1188 vw	(+) w
B	1141 m	(−) s	1138 w	(−) s
A	1093 m	(−) w	1094 m	(−) m
A	1061 m	(+) s	1055 m	(+) s
B	1044 s	(−) m	1049 s	(−) m
B	952 m	(+) m	955 w	(+) w
A	909 s		907 s	(+) vw
B	857 vs		862 vs	(+) m
A	786 vs		785 vs	(+) m
B	736 m		735 m	(−) m
A	632 w		633 w	(−) w
B	~618 w		619 w	(−) w

[a] Reference 2. [b] n.o. = not observed.

chromatographically purified dialdehydes were decarbonylated with $(PPh_3)_3RhCl$,[12] and the enantiomeric d_2-cyclopropanes were purified by preparative gas chromatography (33% yield from a resolved d_2-diester).

Absorption spectra at 1-, 4-, and 8-cm^{-1} resolution were obtained in the range 3100–600 cm^{-1} on a Nicolet 7199 FTIR spectrometer. A 5-cm path length gas cell equipped with KBr windows and a sidearm for condensing the sample was filled to 430 Torr (~26.7 mg sample) for the 1-cm^{-1} resolution spectra. At 1-cm^{-1} resolution, all the fundamentals, with the exception of one very weak mode, could be identified. In general, the 10 vibrational modes of *B* symmetry species have "type A" absorption band contours with an intense Q branch, whereas the 11 modes of *A* symmetry species have "type B" contours characterized by two sharp Q branches on either side of the zero-line and broader P and R branches.[13] The frequencies of the observed modes, listed in Table I, are within a few wavenumbers of the calculation of Lowe et al.[2] using the empirical force field of Duncan and Burns.[14]

VCD spectra above 2000 cm^{-1} were recorded on a dispersive VCD instrument[15] as a sum of 4–8 scans with 10-s time constant and 1 Å/s scan rate. The maximum resolution obtainable with sufficient signal quality was 7.2 cm^{-1} at 3000 cm^{-1} and 5.4 cm^{-1} at 2100 cm^{-1}. VCD spectra between 1600 and 850 cm^{-1} were obtained with a modified Nicolet 7199 FTIR spectrometer[16] at resolutions of 4 and 1 cm^{-1}.

The VCD spectra of the two antipodes in the CD stretching region, shown in Figure 1, demonstrate the expected mirror image VCD intensities; the intensities in this region are dominated by the negative, higher frequency VCD contribution from the weak, unresolved *A* symmetry mode, overlapped by weaker positive VCD intensity for the *B* symmetry CD stretch at lower frequency. From the absorption spectra at 1 cm^{-1} resolution, we estimate that the weak *A* mode is centered at ~2277 cm^{-1}; the intense Q branch of the *B* mode lies at 2269 cm^{-1}. The VCD pattern is in agreement with the signs predicted by the ab initio VCD intensity calculation of Lowe et al.,[2] but the relative intensities, which were calculated to be nearly equal, are not. Due to the low resolution (7.2 cm^{-1}) and the extensive overlap of the four broad fundamental bands in the gas phase, the VCD features in the CH stretching region (not shown), while reproducible, are not readily associated with individual vibrations. The observed pattern can be reasonably generated from individual VCD features with the calculated signs.

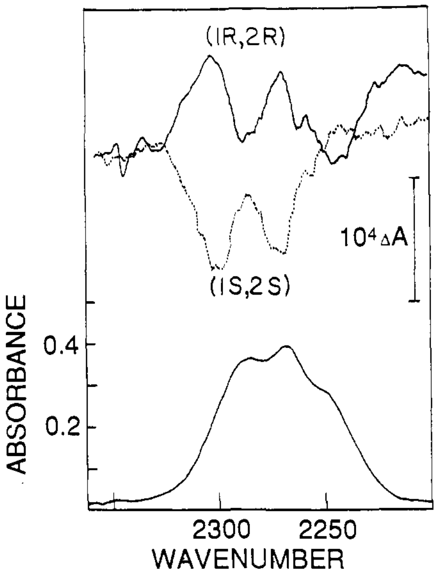

Figure 1. VCD and absorption spectra of (+)-(*S*,*S*)- and (−)-(*R*,*R*)-cyclopropane-1,2-$^2H_2$ in the gas phase (320 Torr, 5-cm path length, 20-mg sample) at 7.2-cm^{-1} resolution. The VCD spectra are the sum of four scans. The instrument was purged with N_2 to eliminate interference from CO_2 absorption.

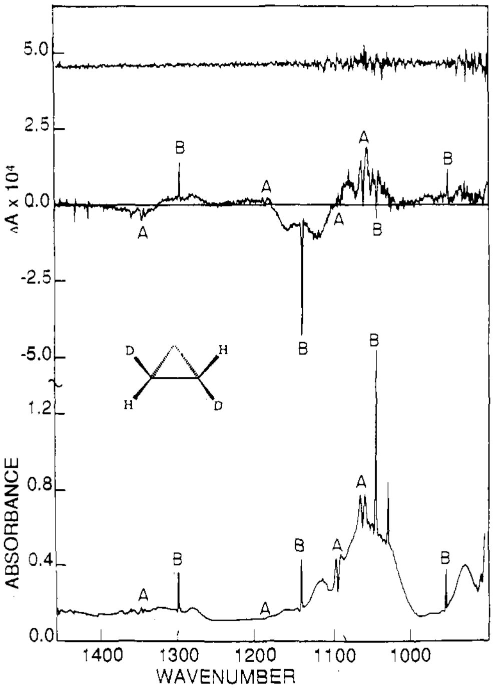

Figure 2. Absorbance (lower trace), VCD (center trace), and VCD noise estimate (upper trace) of (+)-(*S*,*S*)-cyclopropane-1,2-$^2H_2$ in the gas phase at 1-cm^{-1} resolution.

In Figure 2, we present the mid-infrared VCD and absorbance spectra between 1500 and 900 cm^{-1}. The VCD spectrum is the first gas-phase VCD at 1 cm^{-1} resolution to be reported. The spectrum is one half the difference of spectra for the two antipodes, each the sum of 4608 AC and 576 DC scans, accumulated in blocks of 128 AC and 16 DC scans, and requiring an acquisition

---

(12) Decarbonylations of other α-deuteriocyclopropanecarboxaldehydes using Wilkinson's catalyst have been shown to occur with complete retention of stereochemical integrity; see, inter alia; Baldwin, J. E.; Patapoff, T. W.; Barden, T. C. *J. Am. Chem. Soc.* **1984**, *106*, 1421–1426.

(13) Herzberg, G. *Infrared and Raman Spectra of Polyatomic Molecules*; Van Nostrand: Princeton, NJ, 1945; Chapter 4.

(14) Duncan, J. L.; Burns, G. R. *J. Mol. Spectrosc.* **1969**, *30*, 253–265.

(15) (a) Diem, M.; Gotkin, P. J.; Kupfer, J. M.; Tindall, A. G.; Nafie, L. A. *J. Am. Chem. Soc.* **1977**, *99*, 8103–8104. (b) Diem, M.; Gotkin, P. J.; Kupfer, J. M.; Nafie, L. A. *J. Am. Chem. Soc.* **1978**, *100*, 5644–5650. (c) Diem, M.; Photos, E., Khouri, H.; Nafie, L. A. *J. Am. Chem. Soc.* **1979**, *101*, 6829–6837.

(16) (a) Lipp, E. D.; Zimba, C. G.; Nafie, L. A. *Chem. Phys. Lett.* **1982**, *90*, 1–5. (b) Lipp, E. D.; Nafie, L. A. *Appl. Spectrosc.* **1984**, *38*, 20–25.

time of 12 h. At this resolution, individual VCD features with the same contours as the absorption bands are observed for all the modes. At 4-cm^{-1} resolution, band contours for the more isolated bands were reproduced, but the individual contributions from the three modes near 1050 cm^{-1} were not resolved. However, the signal-to-noise ratio was considerably higher at the lower resolution (6144 AC and 384 DC scans for each enantiomer). The signs of the VCD intensities calculated by Lowe et al. agree with the experimental observations at 1-cm^{-1} resolution. In particular, the VCD couplets due to the modes at 1356 (*A*), 1300 (*B*) cm^{-1}, and at 1141 (*B*), 1061 (*A*) cm^{-1} are prominent in both the experiment and calculation.

Acknowledgment. This work was supported by grants from the National Science Foundation (CHE 86-02854 to L.A.N. and T.B.F. and CHE 87-21656 to J.E.B.).

TICT Fluorescence Emission Dependence on Excitation Wavelength for Ethyl *p*-(Dimethylamino)benzoate in Supercritical Trifluoromethane

Bruce J. Hrnjez,[1] Parvin T. Yazdi,[2] Marye Anne Fox,*[,1] and Keith P. Johnston*[,2]

Departments of Chemistry and Chemical Engineering
The University of Texas at Austin
Austin, Texas 78712

Received September 1, 1988

Supercritical fluids[3,4] have only recently been recognized[5,6] for their utility in probing solvent effects on photophysical phenomena. The alluring feature of a supercritical fluid is that a minor perturbation, such as a small change in pressure in the vicinity of the critical point, affords a large change in the density-dependent bulk solvent properties such as dielectric constant and viscosity. Uniquely, then, solvent effects can be probed without change of solvent. We report here the use of supercritical media to examine the highly polarity-dependent formation of the twisted-intramolecular-charge-transfer (TICT)[7] state of ethyl *p*-(dimethylamino)benzoate (**1**).

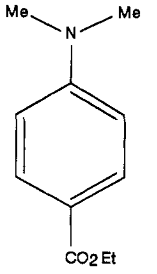

1

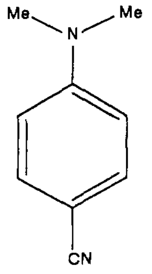

2

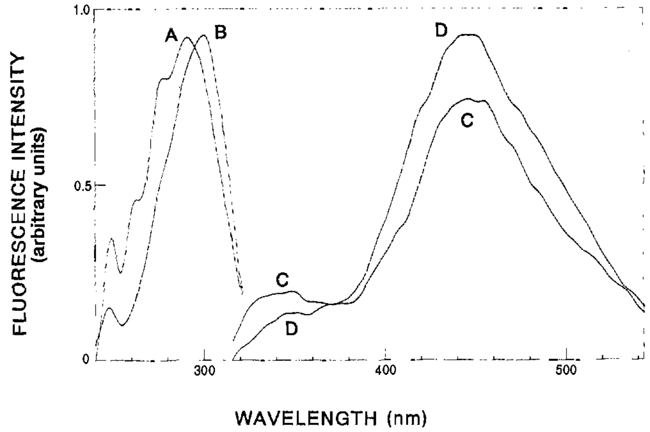

Figure 1. Luminescence dependence on excitation wavelength for ester **1** (10^{-6} M) in CHF_3 at 28 °C and 102.0 bar. Curve A: excitation spectrum monitored at 350 nm; maximum 291 nm. Curve B: excitation spectrum monitored at 434 nm (intensity divided by a factor of five); maximum 300 nm. Curve C: emission spectrum for excitation at 282 nm; maxima 350 and 444 nm. Curve D: emission spectrum for excitation at 298 nm; maximum 446 nm. Curves C and D are corrected for relative absorbance efficiency. Data collected in ratio mode.

We studied the steady-state fluorescence behavior of **1** in CHF_3 (T_c = 25.9 °C, P_c = 46.9 bar) at 28 °C and several pressures ranging from 44.9 to 136.0 bar. The ester **1** was purified by column chromatography and sublimation, and CHF_3 was deoxygenated by freeze–pump–thaw techniques (< 10 ppm O_2) and freed of weakly fluorescent impurities by passage through an in-line activated carbon filter.

Representatively, Figure 1 depicts the luminescence behavior of ester **1** (10^{-6} M) in CHF_3 at 28 °C and 102.0 bar. The emission profile was a strong function of excitation wavelength for all pressures studied at 28 °C. The excitation spectra, monitored at the planar (curve A) and TICT (curve B) emission maxima, were decidedly nonsuperimposable. Excitation at 282 nm enhanced emission from the short wavelength planar state (curve C), whereas excitation at 298 nm enhanced emission from the long wavelength TICT state (curve D). Similar excitation wavelength dependence was observed for ester **1** in CHF_3 at 50 °C but not at 70 °C. Control experiments showed that ester **1** is stable under our experimental conditions.

This dependence was not observed in normal liquid solvents such as n-C_6H_{14}, CH_2Cl_2, $CHCl_3$, and CH_3CN; nor was it observed in the supercritical media CO_2 (35 °C) and C_2H_6 (36 °C) at the many pressures examined. The absence of an excitation wavelength dependence under these conditions indicates that the anomalous dependence in CHF_3 was not due to the presence of an impurity in our sample of ester **1**.

Kajimoto[6] did not report emission dependence on excitation wavelength for the closely related *p*-(dimethylamino)benzonitrile (**2**) in supercritical CHF_3 at 50 °C. We confirmed the absence of excitation wavelength dependence for **2** at 50 °C in CHF_3 and further report that this dependence is absent at 28 °C. These experiments indicate that the presence of an excitation wavelength dependence for **1** in CHF_3 is not due to an impurity in CHF_3 and also suggest that the ester functionality in **1** plays a key role in this dependence phenomenon.

The possibility that deposition of microcrystalline **1** on the emission window or aggregation of **1** in solution could account for the observed excitation energy dependence can be discounted. First, windows of dissimilar materials, both quartz and sapphire, gave identical results. Second, our sample-loading technique precluded initial window deposition. Third, ester **1** is substantially more soluble in CHF_3 than in the nonpolar CO_2 and C_2H_6. If aggregation or deposition were to occur, it would most likely do so in the solvents in which **1** is less soluble.

Several instances[8-11] of luminescence dependence on excitation

---

(1) Department of Chemistry.

(2) Department of Chemical Engineering.

(3) McHugh, M.; Krukonis, V. *Supercritical Fluid Extraction*; Butterworths: Boston, 1986.

(4) Moore, W. J. *Physical Chemistry*; Prentice-Hall, Inc.: Englewood Cliffs, NJ, 1972; pp 23–25.

(5) Okada, T.; Kobayashi, Y.; Yamasa, H.; Mataga, N. *Chem. Phys. Lett.* **1986**, *128*, 583.

(6) Kajimoto, O.; Futakami, M.; Kobayashi, T.; Yamasaki, K. *J. Phys. Chem.* **1988**, *92*, 1347. Kajimoto demonstrated that the fluorescence and absorbance behavior of *p*-(dimethylamino)benzonitrile (**2**) is a useful probe of solute–solvent clustering in supercritical CHF_3. The use of the supercritical medium as a probe of TICT photophysical behavior was a secondary concern. Johnston previously demonstrated, both experimentally and theoretically, that UV absorbance is a very effective tool for examining solute–solvent interactions in supercritical media. See: Kim, S.; Johnston, K. P. *Ind. Eng. Chem. Res.* **1987**, *26*, 1206.

(7) Rettig, W. *Angew. Chem., Int. Ed. Engl.* **1986**, *25*, 971.

(8) Al-Hassan, K. A.; Azumi, T. *Chem. Phys. Lett.* **1988**, *146*, 121.

0002-7863/89/1511-1915$01.50/0 © 1989 American Chemical Society